

UNCLASSIFIED

AD 268 505

*Reproduced
by the*

**ARMED SERVICES TECHNICAL INFORMATION AGENCY
ARLINGTON HALL STATION
ARLINGTON 12, VIRGINIA**



UNCLASSIFIED

NOTICE: When government or other drawings, specifications or other data are used for any purpose other than in connection with a definitely related government procurement operation, the U. S. Government thereby incurs no responsibility, nor any obligation whatsoever; and the fact that the Government may have formulated, furnished, or in any way supplied the said drawings, specifications, or other data is not to be regarded by implication or otherwise as in any manner licensing the holder or any other person or corporation, or conveying any rights or permission to manufacture, use or sell any patented invention that may in any way be related thereto.

CATALOG BY ASTIA

AS AC 100.

268505

268 505

**APPLICATION OF THE RATE DIAGRAM
TECHNIQUE TO THE ANALYSIS AND
DESIGN OF SPACE VEHICLE ON-OFF
ATTITUDE CONTROL SYSTEMS**

H. Patapoff
21 JUNE 1961

62-1-5-
XEROX

ASTIA
DEC 27 1961
RESOLVED
TIPDR A

SPACE TECHNOLOGY LABORATORIES, INC.
P.O. Box 95001, Los Angeles 45, California

~~NO GTS~~

APPLICATION OF THE RATE DIAGRAM TECHNIQUE TO THE
ANALYSIS AND DESIGN OF SPACE VEHICLE ON-OFF
ATTITUDE CONTROL SYSTEMS

H. Patapoff

21 June 1961

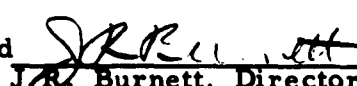
Contract No. AF 33(616)-7811


To be presented at the ARS Guidance and Control Conference
Stanford University, Stanford, California
7-9 August 1961

Approved


R.K. Whitford, Manager
Controls Systems Department

Approved


J.R. Burnett, Director
Electromechanical Laboratory


SPACE TECHNOLOGY LABORATORIES, INC.,
P.O. Box 95001
Los Angeles 45, California

APPLICATION OF THE RATE DIAGRAM TECHNIQUE TO THE
ANALYSIS AND DESIGN OF SPACE VEHICLE ON-OFF
ATTITUDE CONTROL SYSTEMS

H. Patapoff*

ABSTRACT

Preliminary single axis analysis and design of a space vehicle control system, consisting of a torque producing device and a dead-band within which there are no externally or internally applied torques, can be accomplished quite effectively by a simple graphical technique termed the "Rate Diagram" method. Two characteristics of typical space vehicle attitude control problems which make this method effective are the undamped rigid body motion of the vehicle and the associated low angular rates. These characteristics satisfy the two basic assumptions required for the use of this technique; namely, that the vehicle angular acceleration is proportional to the applied torque, and that system transients effectively decay prior to control torque application. The system, exclusive of the vehicle dynamics, can be of any order, thus allowing sensor dynamics, shaping networks, control torque characteristics, etc., to be included.

A "Rate Diagram" is simply a plot of the vehicle angular rate at control torque removal versus the rate at torque application. Information regarding system stability, transient response, and limit cycle behavior can be ob-

* Member of the Technical Staff
Space Technology Laboratories
El Segundo, California

tained directly from such a diagram. This diagram can be constructed with relative ease through the use of the analytical relationships developed and presented in this paper. In addition, these relationships allow the analytical determination of limit cycle amplitude and period.

This graphical method of analysis can be quite effective as a design tool in designing systems to meet specified performance requirements. As system parameters or control torque characteristics are varied, the resulting changes in system behavior can be noted visually by the corresponding changes in the Rate Diagram. The interpretation of a Rate Diagram for analysis and design purposes is discussed, and a detailed treatment of an example space vehicle control system problem to exemplify this technique is included.

INTRODUCTION

On-off reaction control systems have found wide application in the field of space vehicle attitude control. This control method is particularly attractive because of its inherent simplicity and relatively high reliability, being most effective and economical in cases where only relatively small correcting torques are necessary to maintain attitude control - especially in cases where the allowable attitude excursions are relatively large.

The control torque generators may be either torque producing devices which change the total vehicle angular momentum in inertial space, or momentum storage devices which transfer angular momentum between the vehicle and rotating inertias within the vehicle. The most commonly used torque producing devices are of the mass ejection type. Compressed gases, liquid

vaporization, or the more sophisticated ion-generation are examples. The most common momentum storage device is the well known reaction wheel.

One of the basic difficulties associated with such nonlinear control systems is the lack of available analysis or synthesis techniques which are suitable for the practicing control engineer. One approach is to treat the problem as a conventional one applicable, say, to phase plane analysis, ignoring effects which make the problem complicated, such as actuator and sensor dynamics. If there are no serious problems associated with such an over-simplified case, it is then hoped that the results will serve as a sort of first approximation to the "real" solution.

A technique is presented in this paper in which the performance of space vehicle control systems can be analyzed without the need of over-simplifying the control problem. Actuator and sensor dynamics and shaping filters can be included in such an analysis. This technique is, however, based upon two major assumptions; namely, that all transients in the system effectively decay prior to control torque command, and that the vehicle dynamics can be represented as a double integration of the control torque. These two assumptions have, in the past, been valid in numerous space vehicle control problems.

SYSTEM DESCRIPTION

A block diagram of the on-off control system considered appears in Figure 1. I is the moment of inertia of the vehicle, whose angular acceleration is proportional to the control torque, T_c . The vehicle attitude, θ , is sensed and compared with the commanded attitude, θ_c . The resulting error signal is filtered and fed to the switch. The switch has a dead-space of $\pm \theta_D$

and a per-unit hysteresis h . The system operation can be explained with the aid of the phase-plane trajectory of Figure 2. Assume that the vehicle rotates at an angular rate, $\dot{\theta}_0$, and that the output signal of the filter lies within the dead space of the switch. As the vehicle rotates, the angular error increases until the filter output becomes θ_D , at which time switch closure occurs. This corresponds to point 1 of Figure 2. τ_A seconds after switch closure, control torque is applied which tends to reverse the direction of travel, corresponding to point 2. The transportation delay time, τ_A , is assumed to be constant. Control torque is applied to the vehicle until the output of the filter reduces to the value $\theta_D(1-h)$, at which time the switch opens. This corresponds to point 3. Control torque is not removed until τ_R seconds after switch opening, corresponding to point 4. The filter output is again within the dead-space of the switch, and the vehicle rotation has been reversed at a rate, $\dot{\theta}_F$. This sequence is now repeated. If the vehicle rotation has not been reversed after torque removal, then torque will again be applied until reversal of rotation does occur. An example phase-plane trajectory for this occurrence is shown in Figure 3.

The filter is assumed to have a rational algebraic transfer function (with poles in the left half s plane) with unity zero frequency gain. The actuator and sensor dynamics are included in the filter transfer function.

The control torque build-up and tail-off characteristics are assumed to be the same for either positive or negative vehicle accelerations. Figure 4 shows typical torque characteristics for a constant torque generator. For convenience the control torque tail-off characteristics are included in the time delay, τ_R . For the typical case of Figure 4 the tail-off character-

istics are independent of the switch-off time once full torque has been achieved. If shut-off occurs prior to full torque build-up, or, in the general case, if tail-off characteristics are a function of the control torque "on-time", the necessary modification of τ_R vs. control torque "on-time" can be determined experimentally.

THE RATE DIAGRAM

Definition

A rate diagram is simply a plot of the vehicle angular rate at control torque removal, $\dot{\theta}_f$, versus the rate at control torque application, $\dot{\theta}_o$.

Construction

Analytical expressions for use in constructing such a diagram are derived in the Appendix.

Since the control system characteristics, except for sign, are assumed identical for both positive and negative vehicle rotations, it is sufficient to construct rate diagrams only for positive values of $\dot{\theta}_o$. It is sufficient to know only the angular rate at torque removal, $\dot{\theta}_f$, relative to $\dot{\theta}_o$.

Due to the fact that the control torque tends to reverse the direction of travel, the vehicle final angular rate, $\dot{\theta}_f$, for an infinitesimally small positive initial rate, $\dot{\theta}_o$, is negative. Also, if the final rate has the same sign as the initial rate, its magnitude will be less than that of the initial rate. This, in effect, means that the rate curve (for positive $\dot{\theta}_o$) always lies below the line $\dot{\theta}_o - \dot{\theta}_f = 0$.

Interpretation

1. Stability

The stability of the control system can be determined by the addition of the line, $\dot{\theta}_O + \dot{\theta}_F = 0$, (which will be termed the "minus-one" line) to the rate diagram. If the rate curve lies everywhere above this line, the rate amplitude continually decreases, indicating a stable system. If the rate curve lies everywhere below this line, then the rate amplitude continually increases, indicating an unstable system. Example diagrams appear in Figure 5.

In general, the "minus-one" line ($\dot{\theta}_O + \dot{\theta}_F = 0$) will intersect the rate curve, indicating regions of stability and instability. All points of intersection indicate the existence of symmetrical limit cycles, since $\dot{\theta}_F = -\dot{\theta}_O$. Whether these limit cycles are stable or unstable depends upon the manner in which the rate curve intersects the minus-one line. Unsymmetrical limit cycles (where the magnitudes of the initial and final rates are unequal) can be found, if they exist, by constructing lines perpendicular to the minus-one line. If any of these lines intersects the rate curve at more than one point, and if two points of intersection are equidistant from the minus-one line, then an unsymmetrical limit cycle is indicated. Reference to Figure 6b shows that points 1 and 2 correspond to an unsymmetrical limit cycle. The existence and stability of such limit cycle behavior will not be discussed in this paper.

2. Symmetrical Limit Cycles

Consider the example rate diagram of Figure 6a. The two points of

intersection indicate the existence of symmetrical limit cycles. Points 1 and 2 represent a stable and unstable limit cycle, respectively. Considering point 1, a slight decrease in rate amplitude results in a build-up of amplitude, and a slight increase results in a decrease in amplitude. The system, then, undergoes stable oscillations in the vicinity of point 1. For point 2, a slight increase in rate amplitude results in a continual rate build-up, indicating an unstable system for rates above that corresponding to point 2. A slight decrease in rate amplitude results in a rate decrease until point 1 is reached.

The amplitudes of the limit cycle rates can be read directly from the rate diagram. If, however, the limit cycle rate amplitude is of sole interest (assuming knowledge of existence and stability), it can be determined analytically by use of equations (A-13), (A-15), and (A-16) derived in the Appendix.

For example, assuming a step function for the control torque characteristics, the limit cycle rate amplitude, $\dot{\theta}_{LC}$, is determined using equation (A-15):

$$-g \left(\frac{2\dot{\theta}_{LC}}{\lambda_o} - \tau_R \right) = h \theta_D + \dot{\theta}_{LC} \tau_A + \dot{\theta}_{LC} \left(\frac{2\dot{\theta}_{LC}}{\lambda_o} - \tau_R \right) \quad (1)$$

where

$$g(t_o) = -\lambda_o \mathcal{L}^{-1} \left[\frac{F(s)}{s^3} \right]_{t=t_o} \quad (2)$$

Expressing $F(s)$ in the form:

$$F(s) = \frac{A_m s^m + A_{m-1} s^{m-1} + \dots + A_2 s^2 + A_1 s + 1}{B_n s^n + B_{n-1} s^{n-1} + \dots + B_2 s^2 + B_1 s + 1} \quad (3)$$

or:

$$F(s) = \frac{\prod_{i=1}^m (1 + \tau_{z_i} s)}{\prod_{j=1}^n (1 + \tau_{p_j} s)} \quad (4)$$

and expanding $\frac{F(s)}{s^3}$ into partial fractions (assuming that the order of the denominator of $\frac{F(s)}{s^3}$ is greater than that of the numerator):

$$\frac{F(s)}{s^3} = \frac{1}{s^3} + \frac{C_2}{s^2} + \frac{C_1}{s} + \sum_{j=1}^n \frac{K_j}{1 + \tau_{p_j} s} \quad (5)$$

gives:

$$\mathcal{L}^{-1} \left[\frac{F(s)}{s^3} \right] = \frac{t^2}{2} + C_2 t + C_1 + \sum_{j=1}^n \frac{K_j}{\tau_{p_j}} e^{-\frac{t}{\tau_{p_j}}} \quad (6)$$

The partial fraction coefficients of equation (5) can be determined from the following relationships:

$$C_2 = A_1 - B_1 \quad (7)$$

$$C_1 = A_2 - B_2 - B_1 (A_1 - B_1) \quad (8)$$

where:

$$A_1 = \sum_{i=1}^m \tau_{z_i} \quad (9)$$

$$B_1 = \sum_{j=1}^n \tau_{p_j} \quad (10)$$

$$A_2 = \frac{1}{2} \sum_{i=1}^m \sum_{\substack{j=1 \\ i \neq j}}^m \tau_{z_i} \tau_{z_j} \quad (11)$$

$$B_2 = \frac{1}{2} \sum_{i=1}^n \sum_{\substack{j=1 \\ i \neq j}}^n \tau_{p_i} \tau_{p_j} \quad (12)$$

If $F(s)$ contains simple poles:

$$K_j = \left[(1 + \tau_{p_j} s) \frac{F(s)}{s^3} \right]_{s = -\frac{1}{\tau_{p_j}}} \quad (13)$$

$$C_2 = \sum_{j=1}^n \frac{K_j}{(\tau_{p_j})^2} \quad (14)$$

$$C_1 = - \sum_{j=1}^n \frac{K_j}{\tau_{p_j}} \quad (15)$$

Combining equations (1), (2), and (6):

$$\dot{\theta}_{LC} = \frac{1}{2 \left[C_2 - \left(\frac{\tau_A + \tau_R}{2} \right) \right]} \left\{ h\theta_D + \lambda_o \tau_R C_2 - \frac{\lambda_o \tau_R^2}{2} - \lambda_o C_1 - \sum_{j=1}^n \frac{\lambda_o K_j}{\tau_{p_j}} e^{-\frac{t_{LC}}{\tau_{p_j}}} \right\} \quad (16)$$

where:

$$t_{LC} = \frac{2\dot{\theta}_{LC}}{\lambda_o} - \tau_R \quad (17)$$

Assuming simple poles for $F(s)$, and substituting equation (15) into (16):

$$\dot{\theta}_{LC} = \frac{1}{2 \left[C_2 - \left(\frac{\tau_A + \tau_R}{2} \right) \right]} \left\{ h\theta_D + \lambda_o \tau_R C_2 - \frac{\lambda_o \tau_R^2}{2} + \lambda_o \sum_{j=1}^n \frac{K_j}{\tau_{p_j}} (1 - e^{-\frac{t_{LC}}{\tau_{p_j}}}) \right\} \quad (18)$$

If $F(s)$ is simply a pure lead,

$$F(s) = 1 + \tau_1 s \quad (19)$$

then Equation (18) reduces to the algebraic relation:

$$\dot{\theta}_{LC} = \frac{m_o h\theta_D}{2} + \frac{\lambda_o \tau_R}{4} (2 + \tau_A m_o) \quad (20)$$

where

$$m_o = \frac{1}{\tau_1 - \left(\frac{\tau_A + \tau_R}{2} \right)} \quad (21)$$

If $F(s)$ is a lead-lag filter,

$$F(s) = \frac{1 + \tau_1 s}{1 + \tau_2 s} \quad (22)$$

then Equation (18) becomes:

$$\dot{\theta}_{LC} = \frac{m_1 h \theta_D}{2} + \frac{\lambda_o \tau_R}{4} (2 + \tau_A m_1) + \frac{m_1 \lambda_o \tau_2 (\tau_1 - \tau_2)}{2} (1 - e^{-\alpha}) \quad (23)$$

where

$$m_1 = \frac{1}{\tau_1 - \tau_2 - \left(\frac{\tau_A + \tau_R}{2} \right)} \quad (24)$$

$$\alpha = \frac{1}{\tau_2} \left(\frac{2\dot{\theta}_{LC}}{\lambda_o} - \tau_R \right) \quad (25)$$

Since the term, α , in Equation (23) is a function of $\dot{\theta}_{LC}$, a graphical or iterative solution for $\dot{\theta}_{LC}$ is necessary.

The maximum excursion of the vehicle, θ_M , (see Figure 7) is given by the relation:

$$\theta_M = \theta_D + \frac{\dot{\theta}_{LC}^2}{2\lambda_o} - \frac{\dot{\theta}_{LC}}{m} \quad (26)$$

where

$$m = \frac{1}{c_2 - \tau_A} \quad (27)$$

Here, $-m$ is the slope of the control torque "on" line. Because of the assumption that transients effectively decay prior to switch-on, these "on" lines, which intersect the θ axis at $\pm \theta_D$, can be constructed in the phase-plane. The construction of "off" curves, however, become quite tedious.

The period, T_{LC} , of the limit cycle is determined by noting (see Figure 7) that the time interval between points 1 and 2 is simply $\theta_o / \dot{\theta}_{LC}$, where

$$\theta_o = \theta_D - \frac{\dot{\theta}_{LC}}{m} \quad (28)$$

The total "off-time", T_{off} , per cycle is then:

$$T_{off} = 4 \left(\frac{\theta_D}{\dot{\theta}_{LC}} - \frac{1}{m} \right) \quad (29)$$

The time interval between points 2 and 3 is equal to $t_{LC} + \tau_R$, where t_{LC} is the time at switch opening, and is given by equation (17) for the case of a step torque. For the more general case t_{LC} and $\dot{\theta}_{LC}$ are related by:

$$\dot{\theta}_{LC} = -\frac{1}{2} \int_0^{t_{LC} + \tau_R} \lambda(t) dt \quad (30)$$

This expression is obtained from Equation (A-16) by setting $\dot{\theta}_f = -\dot{\theta}_o$.

For a step torque, the total control torque "on-time" per cycle is:

$$T_{on} = \frac{4\dot{\theta}_{LC}}{\lambda_o} \quad (31)$$

This gives a limit cycle period of

$$T_{LC} = T_{on} + T_{off} = 4 \left(\frac{\theta_D}{\dot{\theta}_{LC}} + \frac{\dot{\theta}_{LC}}{\lambda_o} - \frac{1}{m} \right) \quad (32)$$

The total impulse expended by the control system per cycle is equal to $4I\dot{\theta}_{LC}$. The impulse per unit time, which gives a measure of fuel consumption, is then:

$$\text{Impulse/unit time} = \frac{4I\dot{\theta}_{LC}}{T_{LC}} \quad (33)$$

If minimization of fuel consumption during limit cycling is the goal for a specific control problem, this is accomplished analytically by partial differentiation of Equation (33) with respect to the parameter of interest, or graphically by simply plotting Equation (33).

3. Construction of Phase-Plane Trajectories From the Rate Diagram

In order to have a better understanding of the interpretation of a rate diagram, let us construct a typical phase-plane trajectory from the example rate diagram of Figure 8. Let us assume a step control torque and an initial vehicle rotation at an angular rate corresponding to point A of Figure 9. The response of the system for this initial rate will now be followed. The vehicle rate at

switch-off (point B) has a value that is opposite in sign to that corresponding to point A. This means that the vehicle motion has reversed direction. The rate corresponding to B will now remain constant until again switch-on occurs. B, which is now considered the initial rate, gives a final rate, C, at switch-off. C is positive, indicating that the vehicle is still rotating in the same direction, but with a reduced magnitude. After switch-on again occurs, the final rate becomes that corresponding to point D at switch-off. The vehicle has now reversed direction. This is repeated for point E. It is again noted that control torque "on" lines can be constructed in the phase-plane diagram. These lines intersect the θ axis at $\pm \theta_D$, and have a slope of $-m$, where m is determined from equation (27). If $F(s)$ is expressed in the form of Equation (3), or (A-1) of the Appendix, then m is given by:

$$m = \frac{1}{A_1 - B_1 - \tau_A} \quad (34)$$

The slope of the switch-on line is simply $\frac{1}{A_1 - B_1}$

For this special case (step control torque) control torque "off" curves can readily be constructed in the phase-plane, since the trajectories are parabolic. However, in the more general case, where the control torque is a function of time, the construction of these "off" curves becomes rather tedious since the vehicle attitude must be determined at control torque removal. Numerical integration may be necessary.

4. Transient Response

Some general remarks can be made concerning the transient behavior of the system. If the rate curve lies near, and is parallel, or nearly parallel, to the minus-one line, then convergence is relatively slow. Rapidity of convergence increases as the rate curve nears the $\dot{\theta}_0$ axis. Examples appear in Figure 10.

Convergence to the limit cycle for rates in the vicinity of a stable limit cycle depends upon the slope and shape of the rate curve at the intersection with the minus-one line. If the slope of the rate curve approaches + 1 (perpendicular to the minus-one line) at the intersection, convergence becomes slow. Also, if the slope of the curve approaches - 1 (parallel to the minus-one line), convergence becomes slow. Convergence to the limit cycle improves as the slope of the rate curve approaches zero at the point of intersection. Example rate diagrams with corresponding example phase-plane trajectories appear in Figures 11, 12, and 13.

DESIGN APPLICABILITY

Several basic problems arise if a systems approach is taken in the design of a satellite or space vehicle. One is a "proper" choice of the various actuating and sensing combinations which will satisfy the performance requirements of the mission. In general this choice will not be unique. In addition, the determination of "desired" characteristics of the various control system elements, and of "proper" signal processing confronts the control engineer. The choice of a design criterion, from which various control system design configurations can be evaluated, plagues the control

engineer because of the difficulty of divorcing the general problem from the details of the mission and the operational concept, and the difficulty in establishing a set of system "values" or absolute standards which allow system "optimization". Whether this set of values or standards is the "right" one is a rather philosophical problem in itself. Because of these basic difficulties, control systems are not presently designed using such a generalized "rational" synthesis approach. The control engineer is forced to select tentative systems and conduct a performance analysis for each system. A trade-off study is then conducted to compare the relative merits of the tentative systems, and a final design is then chosen. This final choice is in essence an intuitive one, in which the designer utilizes his engineering "judgment" or "feel".

The synthesis applicability of the rate diagram technique presented in this paper is based upon this design approach. If, for specific control system configurations, the effects of important parameter variations upon system performance can be understood with the aid of such diagrams, the control engineer can at least develop a "feel", however crude it may be, for the overall design problem. Experience and engineering judgment are still necessary in the final system design.

EXAMPLE CONTROL SYSTEM

The effects upon system performance of an example control system are shown in rate diagram form (Figures 14, 16, 18, and 20) for four cases of parameter variation.

The nominal system parameters chosen are:

$$\lambda_o = 1.0 \text{ deg/sec}^2 \text{ (step function assumed)}$$

$$\tau_A = \tau_R = 0.05 \text{ sec}$$

$$h\theta_D = 0.1 \text{ deg}$$

$$F(s) = \frac{\tau_1 s + 1}{(\tau_2 s + 1) \left(\frac{s^2}{\omega_n^2} + \frac{\sqrt{2}s}{\omega_n} + 1 \right)}$$

Case 1. - Variation of Lead Time Constant (τ_1)

The effect of filter lead time constant variation upon the rate diagram and limit cycle amplitude are shown in Figures 14 and 15. The filter transfer function for this case is:

$$F(s) = \frac{\tau_1 s + 1}{0.1 \tau_1 s + 1}$$

Case 2. - Variation of Time Delay ($\tau_A = \tau_R$)

The effect of time delay variation upon the rate diagram and limit cycle amplitude are shown in Figures 16 and 17. The filter transfer function for this case is:

$$F(s) = \frac{5s + 1}{.5s + 1}$$

Case 3. - Variation of Hysteresis ($h\theta_D$)

The effect of hysteresis variation is shown in Figures 18 and 19. The filter transfer function is:

$$F(s) = \frac{5s + 1}{.5s + 1}$$

Case 4. - Addition of Quadratic Lag

The effect of adding a quadratic lag to the system is shown in Figures 20 and 21. The filter transfer function is:

$$F(s) = \frac{10s + 1}{(s + 1) \left(\frac{s^2}{\omega_n^2} + \frac{\sqrt{2}s}{\omega_n} + 1 \right)}$$

CONCLUSIONS

The detailed treatment of the example control system shows the effectiveness of this technique in designing space vehicle on-off control systems. As filter parameters or control system characteristics are varied, the design engineer "observes" the resulting changes in system behavior by noting the corresponding changes in the rate diagram. This can give a general "feel" for system optimization in meeting the specified performance requirements of the mission. The limit cycle derivations can readily be applied in cases where fuel consumption during limit cycling is of prime interest.

A general design approach is suggested by specifying the desired rate diagram characteristics and designing a filter which will yield the desired rate diagram, or at least a satisfactory approximation. This filter synthesis would probably require computer techniques.

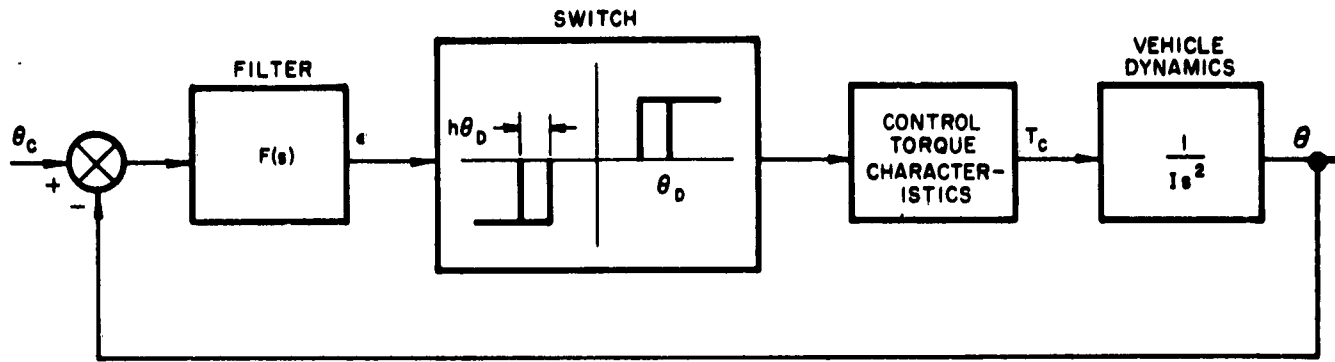


Figure 1. System Block Diagram

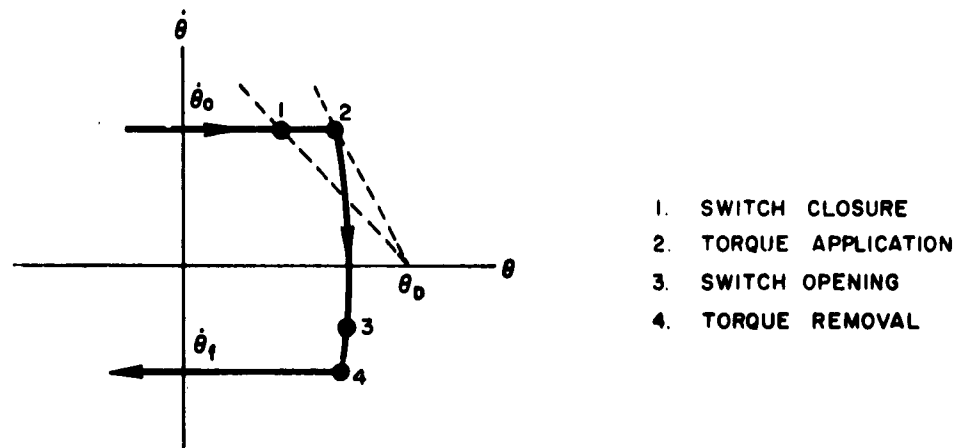


Figure 2. Example Phase-Plane Trajectory

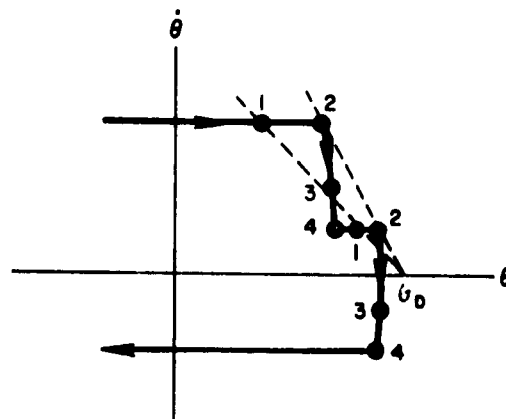


Figure 3. Example Phase-Plane Trajectory

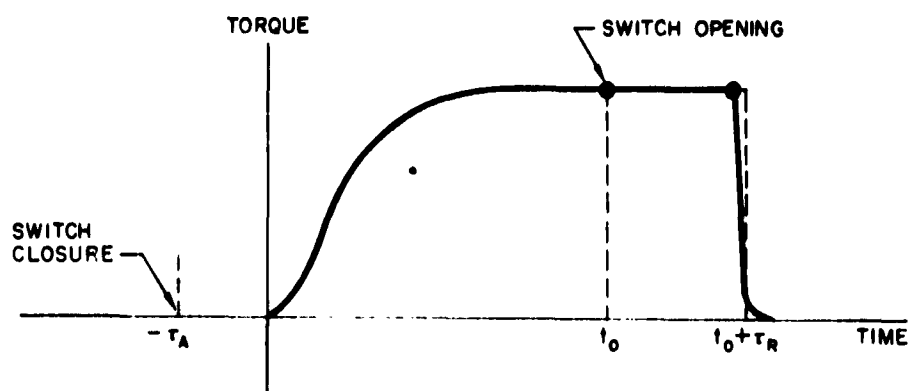


Figure 4. Typical Torque Characteristics

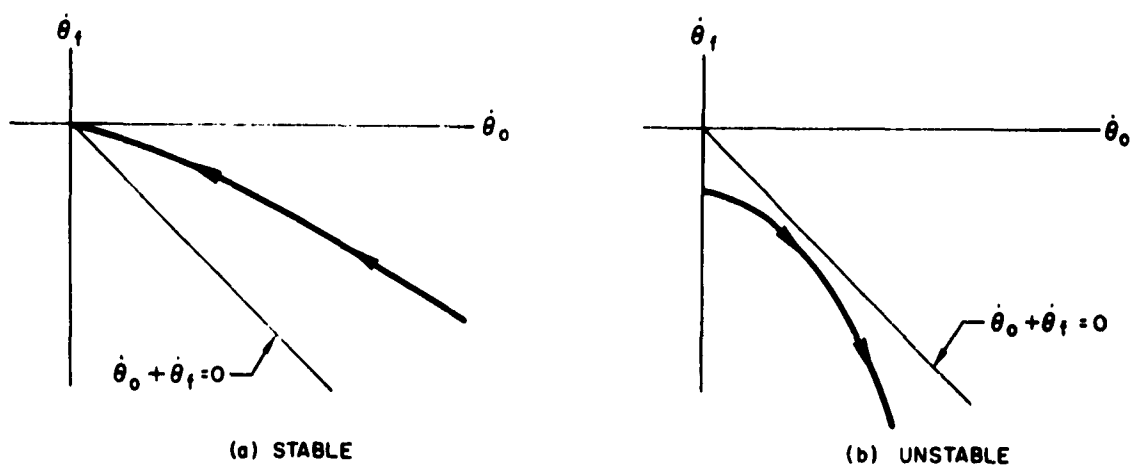


Figure 5. Rate Diagrams Indicating a Stable and Unstable System

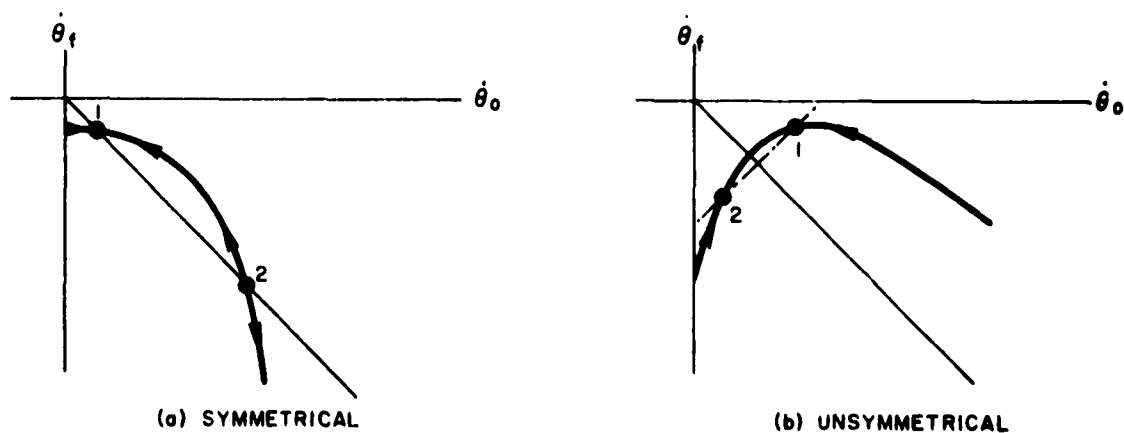


Figure 6. Rate Diagrams Indicating Limit Cycles

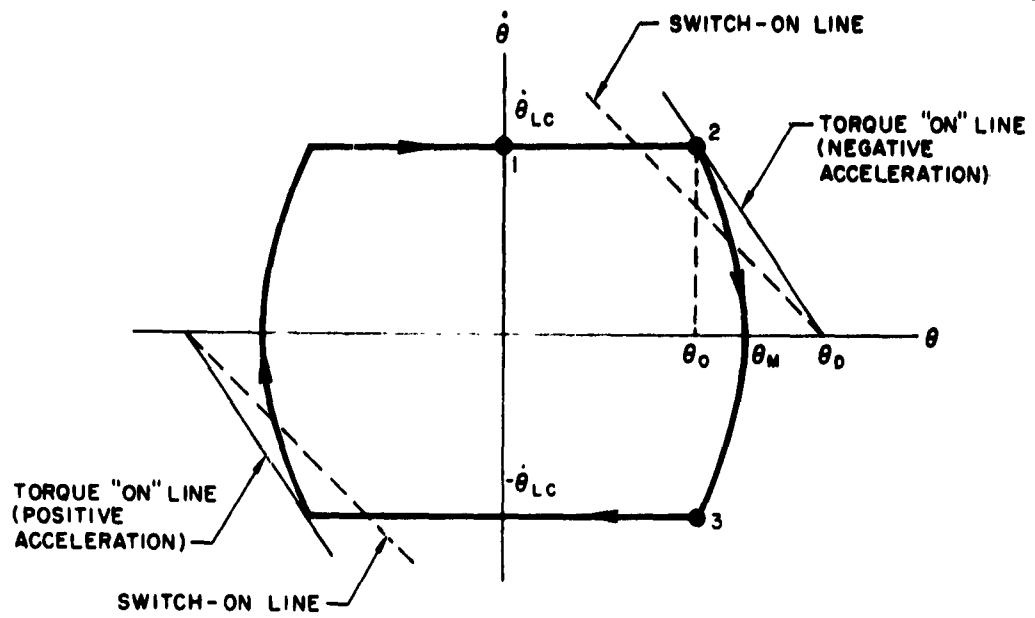


Figure 7. Typical Limit Cycle Phase-Plane Trajectory

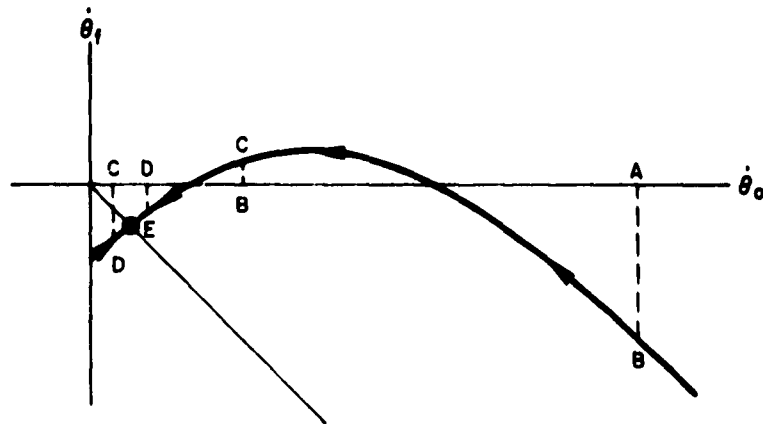


Figure 8. Example Rate Diagram

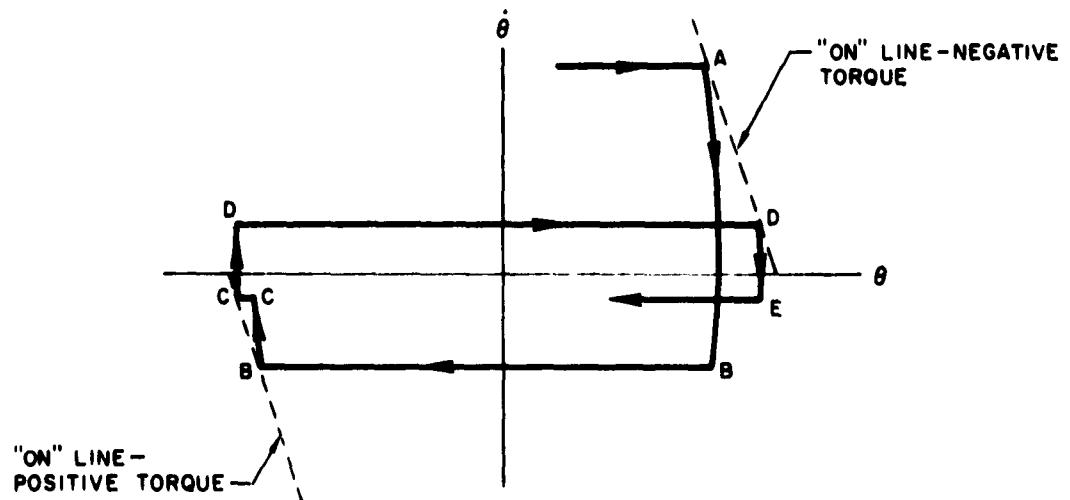


Figure 9. Typical Phase Plane Trajectory for Example System of Figure 8.

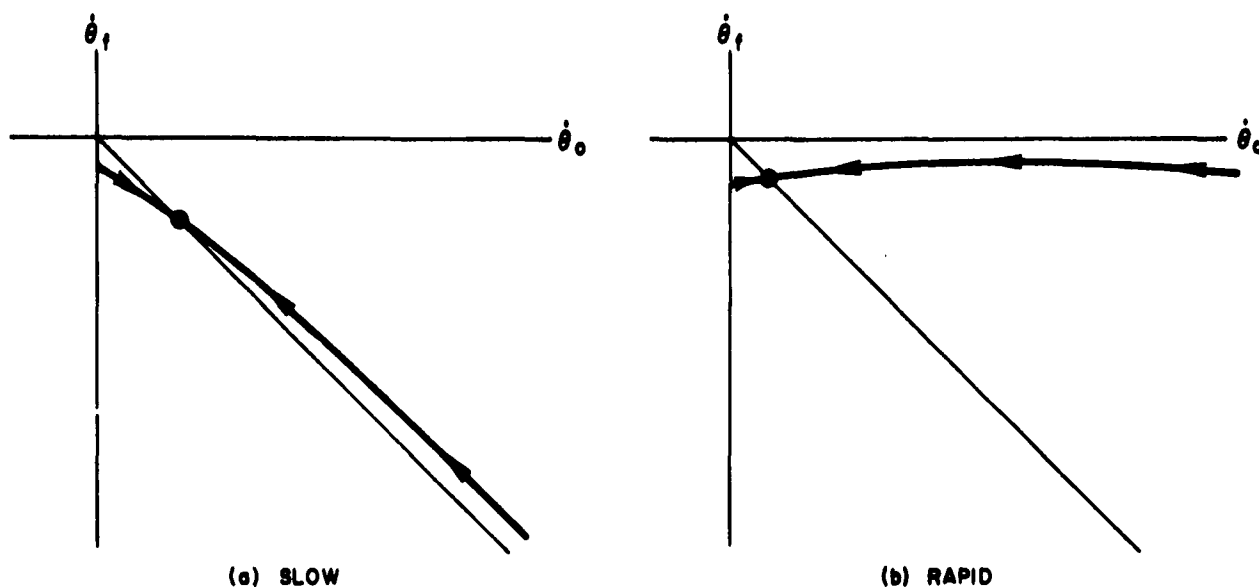


Figure 10. Example Rate Diagrams Indicating Relatively Slow and Rapid Convergence

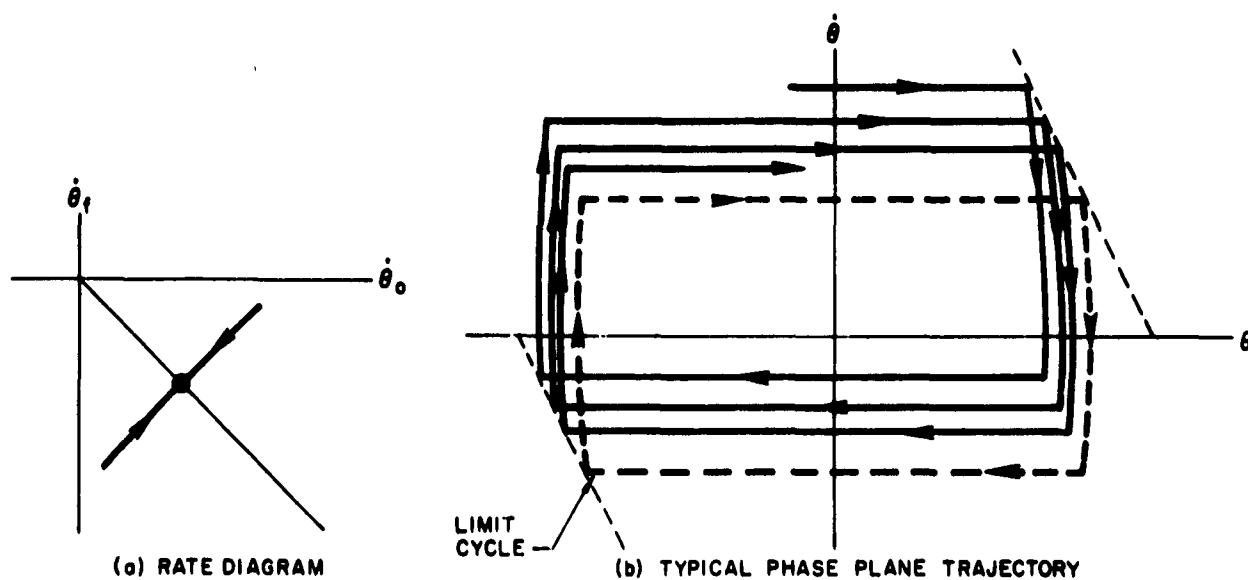


Figure 11. Example Indicating Relatively Slow Convergence In Vicinity of Stable Limit Cycle

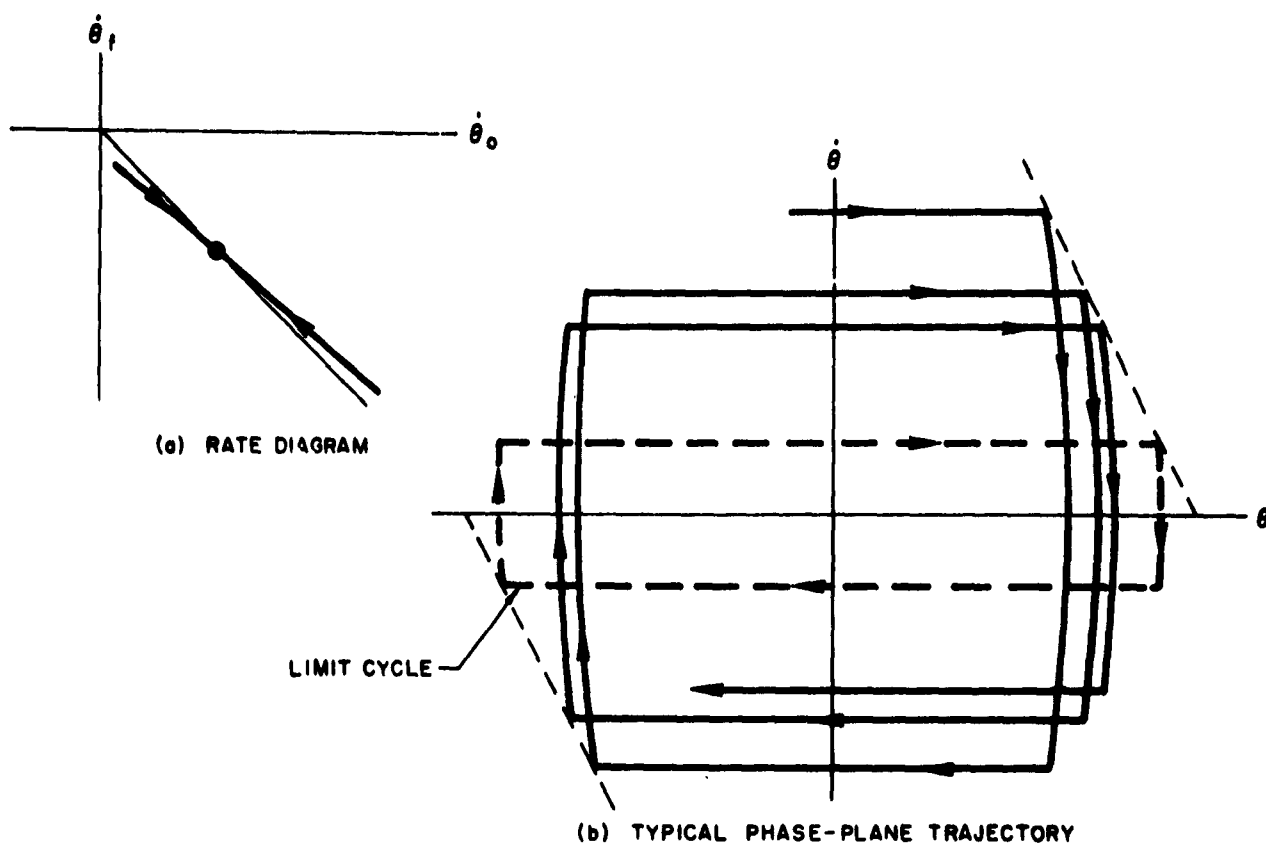


Figure 12. Example Indicating Relatively Slow Convergence
In Vicinity of Stable Limit Cycle

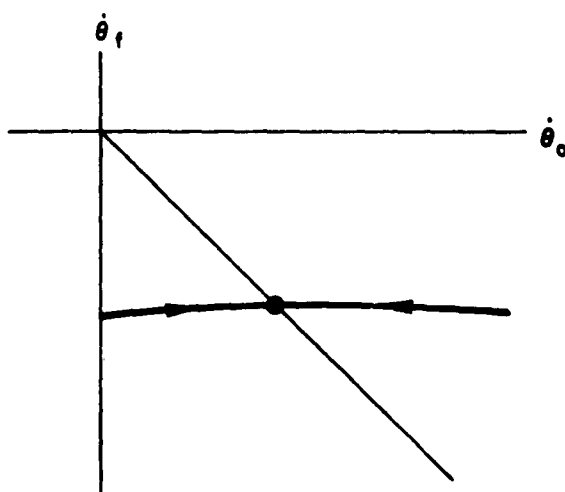


Figure 13. Example Rate Diagram Indicating Rapid Convergence
In Vicinity of Stable Limit Cycle

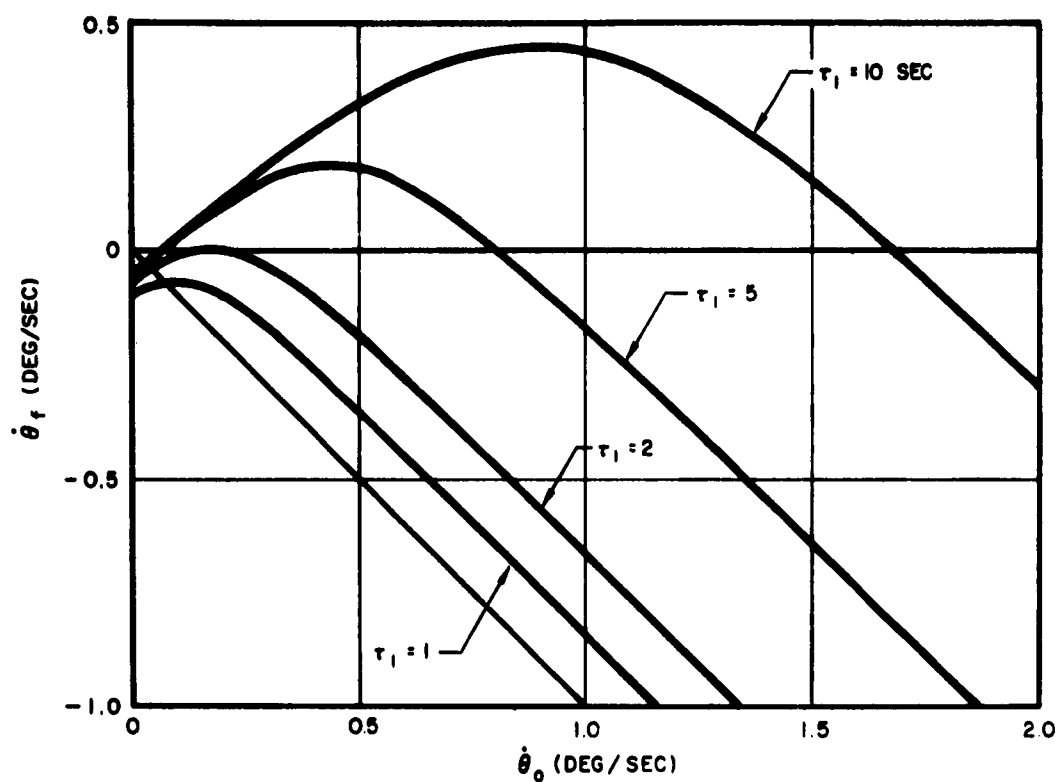


Figure 14. Example Control System Rate Diagrams For Various Values of Lead Time Constant, τ_1

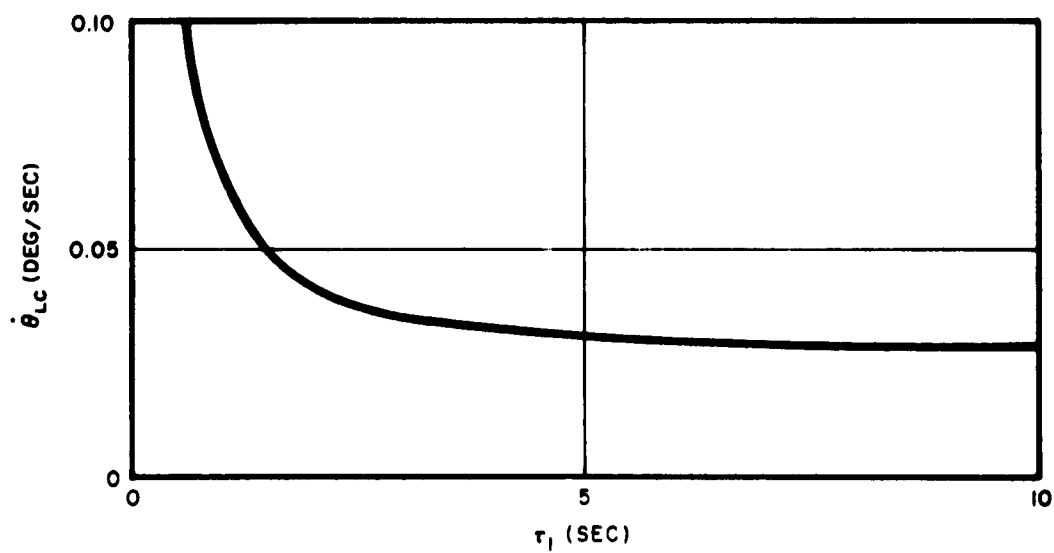


Figure 15. Limit Cycle Rate Amplitude, $\dot{\theta}_{LC}$, vs. Lead Time Constant, τ_1

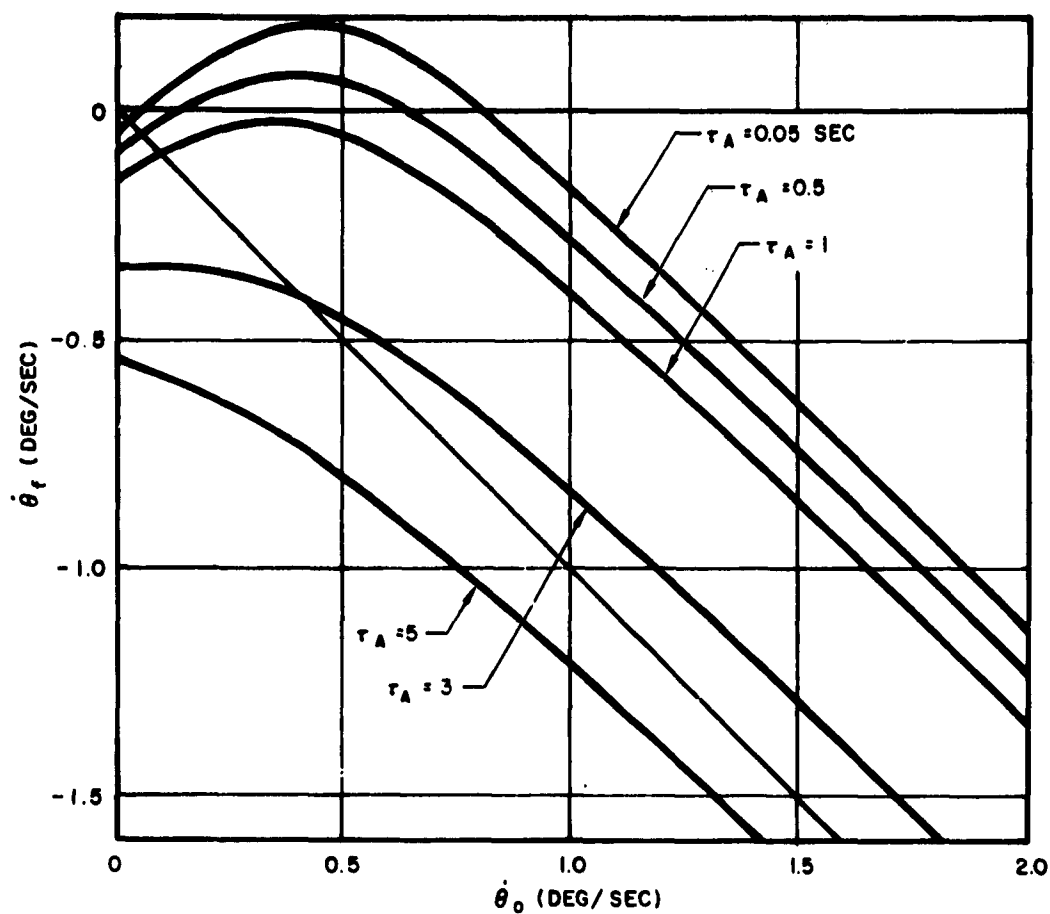


Figure 16. Example Control System Rate Diagrams For Various Values of Time Delay, τ_A (Where $\tau_A = \tau_R$)

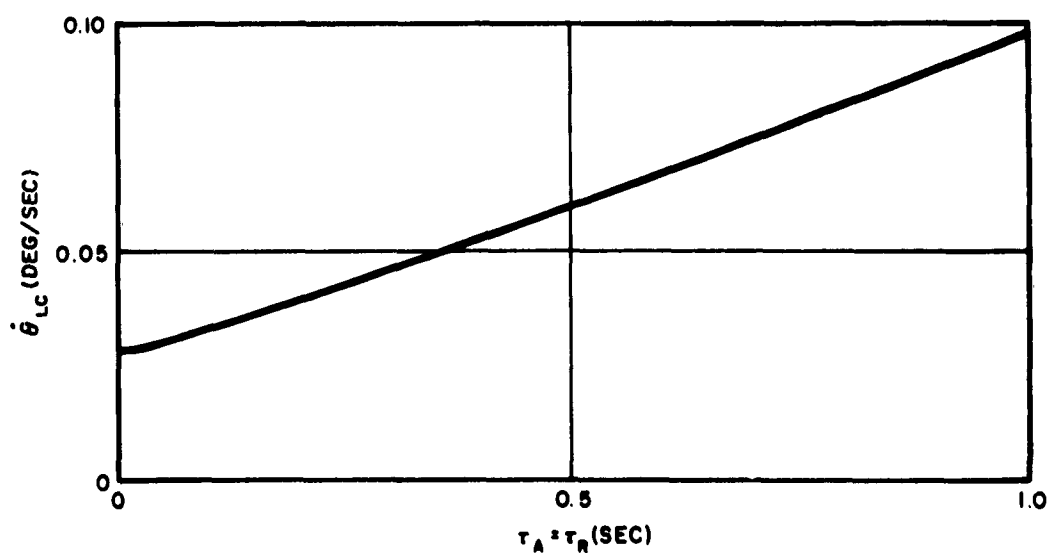


Figure 17. Limit Cycle Rate Amplitude, $\dot{\theta}_{LC}$, vs. Time Delay, τ_A

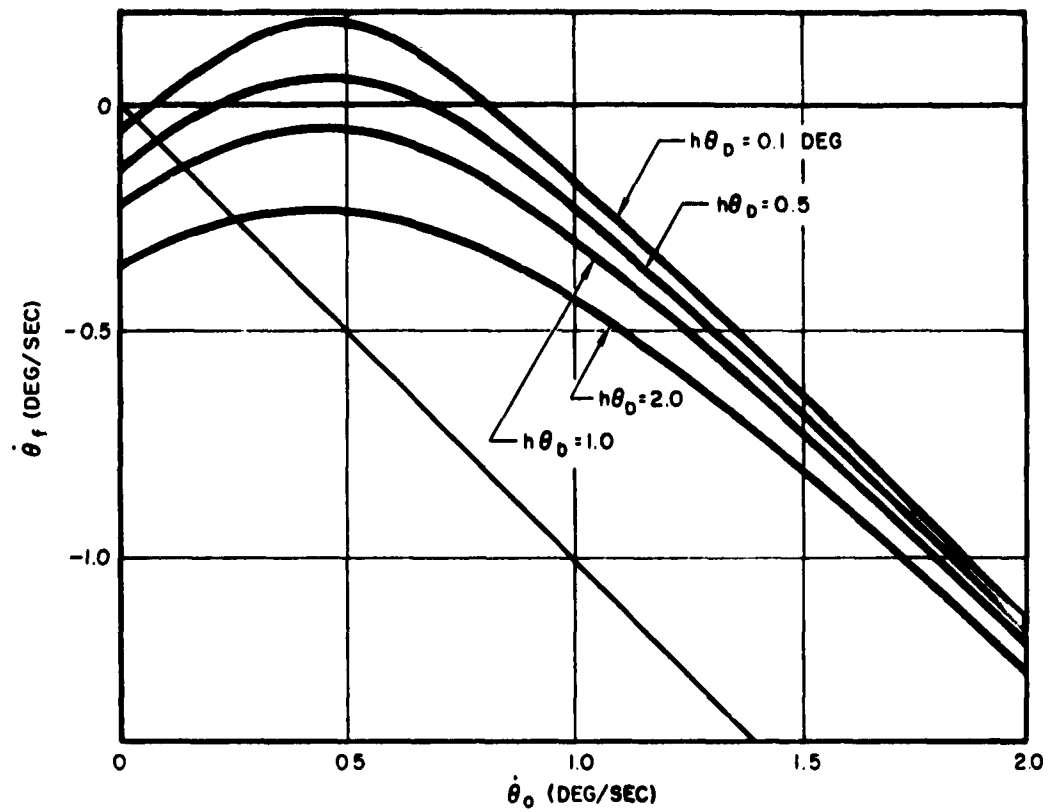


Figure 18. Example Control System Rate Diagrams For Various Values of Hysteresis, $h\theta_D$

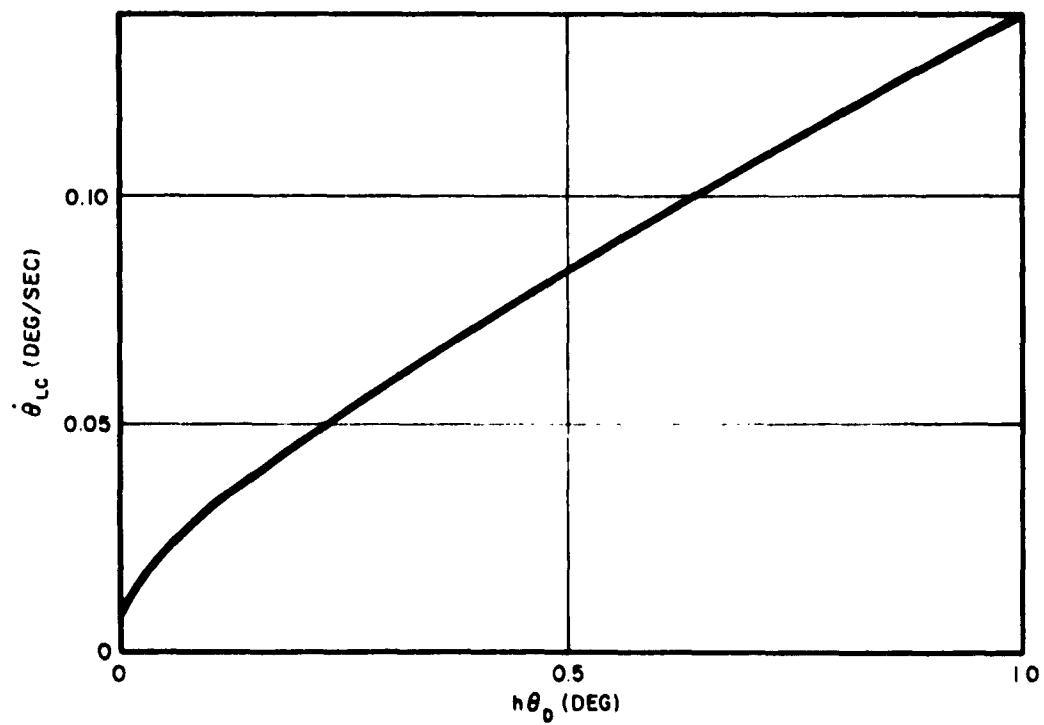


Figure 19. Limit Cycle Rate Amplitude, $\dot{\theta}_{LC}$, vs. Hysteresis, $h\theta_D$

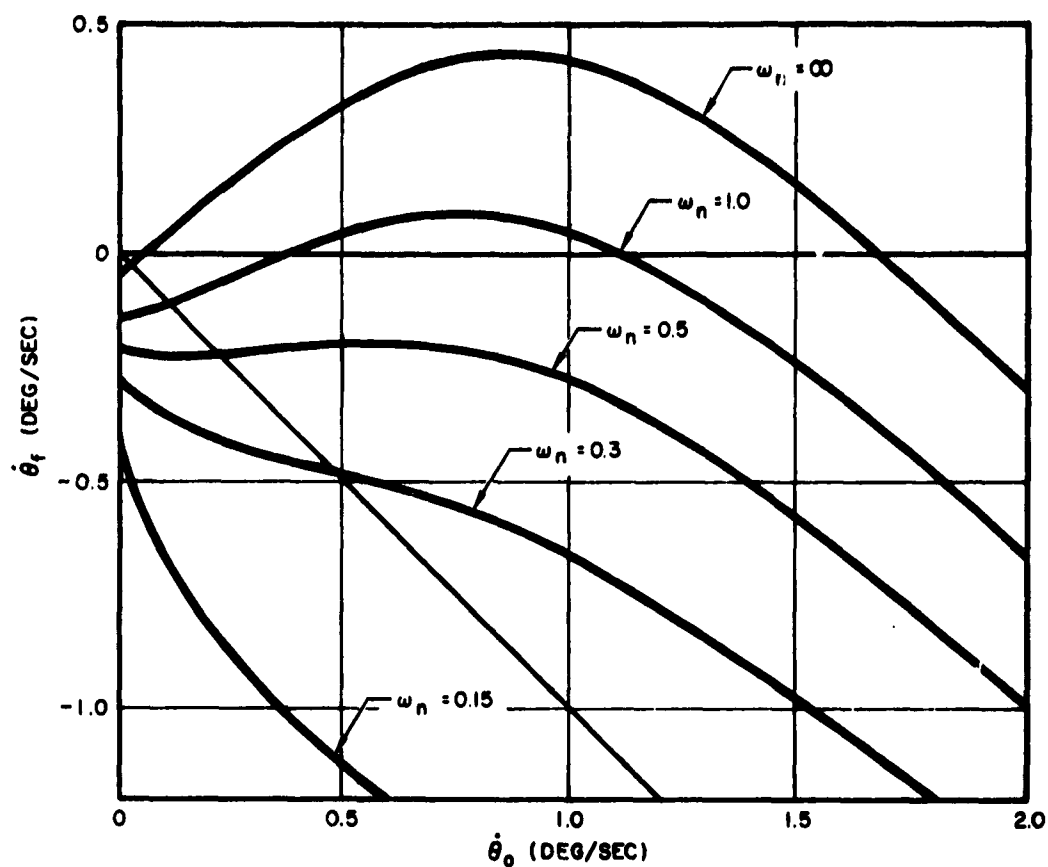


Figure 20. Example Control System Rate Diagrams vs. Quadratic Lag Natural Frequency, ω_n ($\zeta = \frac{\sqrt{2}}{2}$)

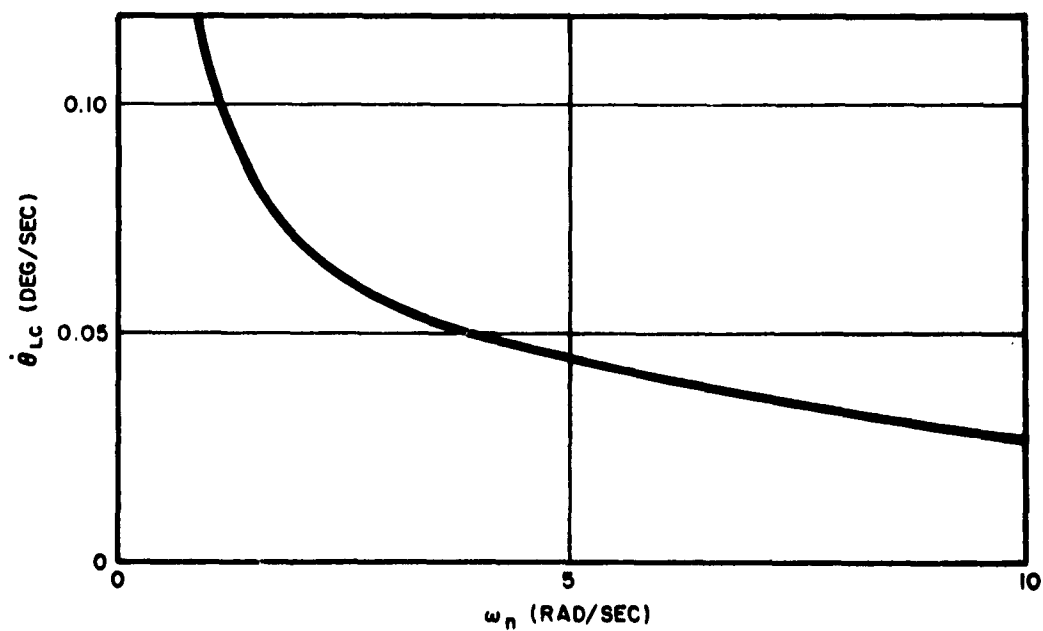


Figure 21. Limit Cycle Rate Amplitude, $\dot{\theta}_{LC}$, vs. Quadratic Lag Frequency, ω_n

APPENDIX

Derivation of Equations for Rate Diagram Construction

Procedure

In constructing a rate diagram an analytical expression relating the vehicle angular rate at control torque removal to the rate at application is first derived. This is accomplished by determining the "on-time" of the control torque, whereby the change in vehicle angular rate can be determined from a knowledge of the torque characteristics. A plot of the rate at torque removal versus the rate at torque application is the rate diagram.

Assumptions

The following derivations are based upon the assumptions that:

1. All transients in the system have effectively decayed prior to switch-on. In other words, the "off-time" of the control torque is long compared to the system time constants.
2. The vehicle dynamics can be represented as a free rigid body in which the acceleration is proportional to the applied torque.
3. The control system characteristics are identical for both positive or negative vehicle rotations.

For simplification, the commanded vehicle attitude, θ_c , is assumed to be zero.

Derivation

Let the filter transfer function, $F(s)$ be expressed as the ratio of the two polynomials:

$$F(s) = \frac{N(s)}{D(s)} = \frac{A_m s^m + A_{m-1} s^{m-1} + \dots + A_1 s + 1}{B_n s^n + B_{n-1} s^{n-1} + \dots + B_1 s + 1} \quad (A-1)$$

Since no torque is applied to the vehicle prior to switch-on, the vehicle rotates at a constant rate, $\dot{\theta}_0$. The filter input, then, is simply a ramp. The steady-state output of the filter, ϵ_{ss} , to the ramp input, $\dot{\theta}_0$, is:

$$\epsilon_{ss} = \left[\theta + (A_1 - B_1) \dot{\theta}_0 \right] \quad (A-2)$$

and

$$\dot{\epsilon}_{ss} = -\dot{\theta}_0. \quad (A-3)$$

It is seen that the filter output leads the input by an amount $\dot{\theta}_0(A_1 - B_1)$, and has the same slope.

Consider the case where switch-on occurs when $\epsilon = -\theta_D$. Control torque application occurs τ_A seconds later, at which time:

$$\epsilon = -(\theta_D + \dot{\theta}_0 \tau_A) \quad (A-4)$$

$$\dot{\epsilon} = -\dot{\theta}_0 \quad (A-5)$$

Now let time begin at control torque application. The differential equation describing the system response is:

$$p^2 D(p) \epsilon(t) = -N(p) \lambda(t) \quad (A-6)$$

where

$$p = \frac{d}{dt}$$

$$\lambda = \frac{T_c}{I}$$

$$T_c = \text{control torque}$$

$$I = \text{vehicle moment of inertia}$$

The initial conditions for the filter output are:

$$\epsilon_o = -(\theta_D + \dot{\theta}_o \tau_A) \quad (A-7)$$

$$\dot{\epsilon}_o = -\dot{\theta}_o \quad (A-8)$$

$$\left. \frac{d^n \epsilon}{dt^n} \right|_{t=0} = 0 \quad \text{for } n > 1 \quad (A-9)$$

Laplace transformation of equation (A-6) then gives:

$$D(s) \left[s^2 E(s) - s \epsilon_o - \dot{\epsilon}_o \right] = -\mathcal{L} \left[N(p) \lambda(t) \right] \quad (A-10)$$

Solving for $E(s)$;

$$-E(s) = \frac{\theta_D + \dot{\theta}_O \tau_A}{s} + \frac{\dot{\theta}_O}{s^2} + \frac{\mathcal{L}[N(p) \lambda(t)]}{s^2 D(s)} \quad (A-11)$$

Then:

$$- \epsilon(t) = \theta_D + \dot{\theta}_O \tau_A + \dot{\theta}_O t + g(t) \quad (A-12)$$

where

$$g(t) = \mathcal{L}^{-1} \left\{ \frac{\mathcal{L}[N(p) \lambda(t)]}{s^2 D(s)} \right\} \quad (A-13)$$

If $\lambda(t)$ is a step function of magnitude λ_O , then:

$$g(t) = - \lambda_O \mathcal{L}^{-1} \left[\frac{F(s)}{s^3} \right] \quad (A-14)$$

Now switch-off will occur when $\epsilon(t) = - \theta_D(1-h)$. Substituting this into equation (A-12) gives:

$$g(t) = - (h\theta_D + \dot{\theta}_O \tau_A + \dot{\theta}_O t) \quad (A-15)$$

The control torque "on-time" is equal to the time, t_O , which satisfies equation (A-15) for the given value of $\dot{\theta}_O$, plus the time delay, τ_R . The switch "on-time" is $t_O + \tau_A$.

The vehicle rate at torque removal, $\dot{\theta}_f$, is given by:

$$\dot{\theta}_f = \dot{\theta}_O + \int_0^{t_O + \tau_R} \lambda(t) dt \quad (A-16)$$

For $\lambda(t)$ a step function of magnitude λ_0 :

$$\dot{\theta}_f = \dot{\theta}_0 - \lambda_0 (t_0 + \tau_R) \quad (A-17)$$

For a given value of $\dot{\theta}_0$, t_0 can be determined from equation (A-15) directly, if the expression for $g(t)$ is simply enough, by iterative methods otherwise, or graphically by plotting $g(t)$ versus time and constructing the line represented by the right hand side of equation (A-15) - the solution being the intersection of the two plots. An indirect, but more convenient method, however, is to treat t_0 as the variable. For a given value of t_0 , $\dot{\theta}_0$ is evaluated using equation (A-15). For this value of t_0 and the corresponding value of $\dot{\theta}_0$, $\dot{\theta}_f$ is determined from equation (A-16). $\dot{\theta}_f$ can then be plotted versus $\dot{\theta}_0$, yielding the rate diagram.